International Journal of Legal Medicine
https://doi.org/10.1007/s00414-019-02141-x

ORIGINAL ARTICLE

Functional characterization of a novel *SCN5A* variant associated with long QT syndrome and sudden cardiac death

Jacqueline Neubauer[1] · Zizun Wang[2] · Jean-Sébastien Rougier[2] · Hugues Abriel[2] · Claudine Rieubland[3] · Deborah Bartholdi[3] · Cordula Haas[1] · Argelia Medeiros-Domingo[4,5]

Received: 18 March 2019 / Accepted: 6 August 2019

Abstract

Sudden arrhythmic death syndrome (SADS) in young individuals is a devastating and tragic event often caused by an undiagnosed inherited cardiac disease. Although post-mortem genetic testing represents a promising tool to elucidate potential disease-causing mechanisms in such autopsy-negative death cases, a variant interpretation is still challenging, and functional consequences of identified sequence alterations often remain unclear. Recently, we have identified a novel heterozygous missense variant (N1774H) in the $Na_v1.5$ channel-encoding gene *SCN5A* in a 19-year-old female SADS victim. The aim of this study was to perform a co-segregation analysis in family members of the index case and to evaluate the functional consequences of this *SCN5A* variant. Functional characterization of the *SCN5A* N1774H variant was performed using patch-clamp techniques in TsA-201 cell line transiently expressing either wild-type or variant $Na_v1.5$ channels. Electrophysiological analyses revealed that variant $Na_v1.5$ channels show a loss-of-function in the peak current densities, but an increased late current compared to the wild-type channels, which could lead to both, loss- and gain-of-function respectively. Furthermore, clinical assessment and genetic testing of the relatives of the index case showed that all N1774H mutation carriers have prolonged QT intervals. The identification of several genotype and phenotype positive family members and the functional implication of the *SCN5A* N1774H variant support the evidence of the in silico predicted pathogenicity of the here reported sequence alteration.

Keywords Sudden arrhythmic death syndrome · Long QT syndrome · *SCN5A* · Exome sequencing · Patch-clamp analysis · Co-segregation analysis

Introduction

Sudden death in the young is a devastating and tragic event. Although a comprehensive medico-legal investigation can identify a clear cause of death in the majority of these cases, up to 30 % of the death remain elusive and are therefore termed as sudden unexplained death [1, 2]. A significant percentage of these young sudden death victims are caused by lethal and potentially heritable cardiac channelopathies or cardiomyopathies, not detectable during conventional autopsy procedures, so-called sudden arrhythmic death syndrome (SADS) [3]. In the last years, several studies applying whole-exome sequencing (WES) and targeted gene analysis identified underlying cardiac diseases in up to 30 % of sudden unexplained death cases [4–10], demonstrating the importance of post-mortem genetic testing in otherwise autopsy-negative unexplained death cases. Nowadays, the challenge of a molecular autopsy is not the identification of variants, but the interpretation of the vast amount of data. Accurate variant classification is crucial to enable proper counselling of

Jacqueline Neubauer and Zizun Wang contributed equally to this work.

Electronic supplementary material The online version of this article (https://doi.org/10.1007/s00414-019-02141-x) contains supplementary material, which is available to authorized users.

✉ Jacqueline Neubauer
jacqueline.neubauer@irm.uzh.ch

[1] Zurich Institute of Forensic Medicine, University of Zurich, Zurich, Switzerland

[2] Institute of Biochemistry and Molecular Medicine, University of Bern, Bern, Switzerland

[3] Department of Pediatrics, Division of Human Genetics, Inselspital, University of Bern, Bern, Switzerland

[4] Department of Cardiology, Inselspital, University Hospital Bern, Bern, Switzerland

[5] Swiss DNAlysis, Dübendorf, Switzerland

Published online: 27 August 2019

surviving family members [11]. Erroneously or prematurely adjudicating ambiguous variants as pathogenic has the potential to unsettle patients and their families [12]. Consequently, co-segregation studies and in vitro functional validation assays are strongly required for an evidence-based classification of the pathogenicity of variants [13].

Recently, we have identified a novel heterozygous missense variant in the sodium voltage-gated channel α-subunit type 5 encoding gene *SCN5A* in a 19-year-old female SADS victim [14]. In this case report, the aim was to perform a co-segregation analysis in family members and to evaluate the functional consequences of the *SCN5A* N1774H variant by electrophysiological recordings.

Materials and methods

Ethical approval for this study was provided by the Cantonal Ethics Committee Zurich (KEK-ZH-Nr. 2013-0086), and the study was conducted in full conformance with the principles of the "Declaration of Helsinki" and with Swiss laws and regulations. All available family members signed an informed consent form for co-segregation analysis and gave approval for publication of this case report (Cantonal Ethics Committee Bern (KEK-BE-Nr. 2016-01602)).

Index case

A 19-year-old woman (weight, 68.4 kg; height, 179 cm; European origin) gave birth to her first child 2 months before she died. She had a minor cough but was otherwise healthy when she suddenly collapsed at her home. The ambulance transferred her to the hospital where, after the diagnosis of irreversible brain damage, life-sustaining measures were stopped. A comprehensive autopsy investigation was performed at the Zurich Institute of Forensic Medicine in Switzerland, according to standard forensic procedures, including pharmacological, toxicological and histopathological screening tests. Autopsy investigation showed a broadening and fat-infiltrated right ventricle and the heart was slightly enlarged (300 g). Pharmacological-toxicological screening tests were negative for drugs and alcohol.

Post-mortem genetic testing (whole-exome sequencing, WES) of the 19-year-old woman has previously been performed within a proof-of-concept study of five young sudden unexplained death cases [14]. The deceased carried a sequence variant in the C-terminus of *SCN5A* (NM001099404.1, Chr3:g.38592543T>G, c.5320A>C, N1774H), which was not previously reported in the literature or in public population databases (Fig. 1). The variant was evaluated according to the recommendations of the American College of Medical Genetics (ACMG) standards and guidelines for the interpretation of sequence variants [13]. Several in silico protein prediction tools (SIFT, MutationTaster, Poly-Phen2, MAPP, Grantham distance score, and AGVGD) predicted the amino acid replacement as probably damaging to the protein structure and function. In addition, the variant is located in a highly conserved region across several species. The *SCN5A* sequence alteration was classified as a variant of unknown significance (VUS), as co-segregation and functional studies had not yet been performed. A second missense variant was located in *SCN5A* (NM_001099404.1, rs1805124, c.1673A>G, H558R). This variant is described as a disease-associated polymorphism with conflicting pathogenicity [15]. Both *SCN5A* variants have been submitted to the Leiden Open Variation Database (ID: 00225626) (https://databases.lovd.nl/shared/individuals/00225626).

Mutagenesis

The variant *SCN5A* N1774H and the deletion of the three amino acids 1505-KPQ-1507 (ΔKPQ) were generated using the plasmid coding for the human $Na_v1.5$ channel and the commercial mutagenesis kit Q5® Site-Directed Mutagenesis Kit from New England BioLabs®inc according to the manufacturer's protocol. The ΔKPQ mutation was used as a positive control due to the described conduction abnormalities leading to QTc prolongation [16]. All the variants were verified by sequencing of the full-length coding sequence.

Cell culture and transfection

TsA-201 cells (ATCC: 96121229) were cultured at 37 °C with 5 % CO_2 in DMEM medium (Gibco, Fisher Scientific, Zurich, Switzerland) and 10 % heat-inactivated foetal bovine serum. For electrophysiological experiments, TsA-201 cells up to passage P20 were transiently transfected with 600 ng cDNA plasmids of interest in 35-mm petri dishes by using JetPEI (Polyplus, 101-10N). The cDNA plasmids of interest were human voltage-gated cardiac sodium channel hSCN5A wild-type (WT), hSCN5A ΔKPQ and hSCN5A N1774H. For the electrophysiological recordings, to mimic the homozygous state, TsA-201 cells were transfected either with hSCN5A WT or N1774H. To mimic the heterozygous state, cells were co-transfected with hSCN5A WT and N1774H at a ratio of 1:1. Additionally, all transfections included 300 ng pIRES-hβ1-CD8 cDNA, encoding the hβ1 subunit and CD8 antigen as a reporter gene. The ratio of JetPEI and total cDNA was 1:3.

Electrophysiological recordings

Patch-clamp recordings, in a whole-cell configuration, were performed at room temperature (24 ± 1 °C) in transiently transfected TsA-201 cells. The VE-2 amplifier (Alembic Instruments Inc., Montreal, Canada) was used for the main biophysical properties (I–V relationship, activation, and

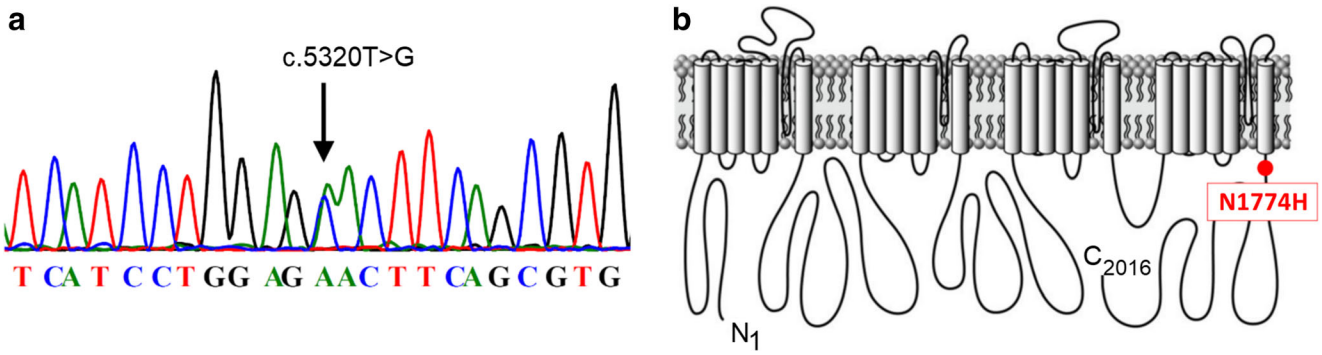

Fig. 1 Genetic analysis of the *SCN5A* N1774H variant. **a** Sanger sequencing of the C-terminus of *SCN5A* confirms the presence of a novel missense variant in the index case resulting in the N1774H substitution. **b** The topology of the $Na_v1.5$ channel and the position of the variant

steady-state inactivation) in the homozygous state and the Axopatch 200B amplifier (Molecular devices, Berkshire, United Kingdom) for the late current recordings. The same Axopatch amplifier was used for the main biophysical properties in the heterozygous state. Currents were filtered at 5 kHz with the Hum Bug lowpass filter (Quest Scientific, North Vancouver, Canada).

For the main biophysical properties in the homozygous state, TsA-201 cells were bathed with a solution containing 50 mmol/L NaCl, 80 mmol/L NMDG-Cl, 2 mmol/L $CaCl_2$, 1.2 mmol/L $MgCl_2$, 5 mmol/L CsCl, 10 mmol/L HEPES and 5 mmol/L glucose (pH was adjusted to 7.4 with CsOH). Pipettes (tip resistance 1.5 to 2.5 MΩ) were filled with a solution containing 60 mmol/L CsCl, 70 mmol/L Cs-Asp, 1 mmol/L $MgCl_2$, 10 mmol/L HEPES, 11 mmol/L EGTA and 5 mmol/L MgATP (pH was adjusted to 7.2 with CsOH).

For the late current, TsA-201 cells were bathed with a solution containing 130 mmol/L NaCl, 5 mmol/L $CaCl_2$, 1 mmol/L $MgCl_2$, 5.6 mmol/L CsCl, 10 mmol/L HEPES and 11 mmol/L glucose (pH was adjusted to 7.4 with NaOH). Pipettes (tip resistance 1.5 to 2.5 MΩ) were filled with a solution containing 60 mmol/L CsCl, 70 mmol/L Cs-Asp, 1 mmol/L $MgCl_2$, 10 mmol/L HEPES, 11 mmol/L EGTA and 5 mmol/L MgATP (pH was adjusted to 7.2 with CsOH). For the main biophysical properties in the heterozygous state, the bath solution contained 25 mmol/L NaCl, 105 mmol/L NMDG-Cl, 2 mmol/L $CaCl_2$, 1.2 mmol/L $MgCl_2$, 5 mmol/L CsCl, 10 mmol/L HEPES and 5 mmol/L glucose (pH was adjusted to 7.4 with CsOH). Pipettes (tip resistance 1.5 to 2.5 MΩ) were filled with the same solution as described earlier.

Data were acquired and analysed with the Axon™ pCLAMP™ 10 Electrophysiology Data Acquisition & Analysis Software, Version 10.7.0.3 (Axon Instruments, Union City, CA, USA) and GraphPad Prism 7, version 7.01 (GraphPad Software, San Diego, CA, USA).

Sodium current densities (pA/pF) were calculated dividing the peak current by the cell capacitance. I–V relationship (IV) were fitted with the following equation: $y = (G_{max}(Vh\text{-}V_{rev},Na))/(1 + \exp.[(Vh–V50)/k])$, in which y is the normalized peak current (pA/pF) at a given holding potential (Vh), V50 is the voltage at which half of the channels are activated, k is the slope factor and G_{max} is the maximum conductance. Steady-state activation (SSA) and steady-state inactivation (SSI) curves were fitted with the following single Boltzmann equation: $y = 1/(1 + \exp.[(Vh–V50)/k])$, in which y is the normalized conductance (SSA) or peak current (SSI) at a given holding potential (Vh), V50 is the voltage at which half of the channels are activated (V50, act) or inactivated (V50, inact) respectively, and k is the slope factor.

A late sodium current percentage was calculated by dividing the non-tetrodotoxin subtracted inward current at a 200-ms post-stimulation by the peak current value. The protocol performed to quantify the late sodium current has been previously published to investigate sodium channel gating under non-equilibrium conditions [17]. This protocol consists of a single sweep containing a step pulse from the holding potential at − 100 mV until + 20 mV during 100 ms. Then a ramp from + 20 mV until − 100 mV during 100 ms. Ten sweeps have been averaged. The time between each sweep was 3 s. The late current has been measured at the end of the step pulse (corresponding at 200 ms) and divided by the peak current recorded at the beginning of the step pulse.

Cell surface biotinylation assay

Following 48 h of incubation, transiently transfected TsA-201 cells were treated with 0.5 mg/ml EZ-link™ Sulfo-NHS-SS-Biotin (BioVision, 2323-100) diluted in cold 1× PBS for 15 min at 4 °C. Then the cells were washed twice with 200 mM glycine in cold 1× PBS and twice with cold 1× PBS to inactivate and remove the remaining biotin, respectively. The cells were lysed for 1 h at 4 °C with 1× lysis buffer consisting of (50 mM HEPES (pH was adjusted to 7.4), 150 mM NaCl, 1.5 mM $MgCl_2$, 1 mM EGTA (pH 8); 10% glycerol, 1 % Triton X-100, 1× Complete Protease Inhibitor Cocktail (Roche, 34,045,200). Cell lysates were centrifuged at 13,200 rpm at 4 °C for 15 min. Two milligrammes of the supernatant were incubated with 50 µl Streptavidin Sepharose High Performance beads (GE Healthcare, 17-5113-01) for 2 h at 4 °C. The beads were subsequently washed three times with 1× lysis buffer and eluted at

37 °C for 30 min with 30 µl of 2× NuPAGE sample buffer (Invitrogen, NP0007) plus 100 mM DTT. The input fractions were re-suspended with 4× NuPAGE Sample Buffer plus 100 mM DTT, yielding a final protein concentration of 2 mg/ml, and then incubated at 37 °C for 30 min.

Western blot

Protein samples were loaded on precast 4–12 % Bis-Tris polyacrylamide gradient gels (Invitrogen, NP0322BOX), transferred with the Trans-Blot Turbo Transfer system (Bio-Rad, Cressier, Switzerland) and detected by the SNAP i.d.® 2.0 detection system (Millipore, C73105) with the following antibodies: anti-α-actin (Sigma, A2066), anti-$Na_v1.5$ (peptide sequence NH_2-DRLPKSDSEDGPRALNQLSC-$CONH_2$ generated by Pineda, Berlin, Germany) and anti-Na/K ATPase (Abcam, ab7671). All pictures were taken by the Li-Cor Odyssey Infrared Imaging System (LI-COR Biosciences GmbH, Bad Homburg, Germany) and further processed with the Li-Cor Image Studio Software lite v.5.2 (LI-COR Biosciences GmbH).

Data analysis and statistical methods

Whole-cell patch-clamp samples were collected on at least three individual transfections. The investigator was sightless to the samples before the data was analysed. A second investigator re-produced the results using blinded samples. Data are presented as the mean ± SEM. A statistical significance was calculated with the GraphPad Prism 7, version 7.01 (GraphPad Software) by either a two-tailed Student *t* test or ANOVA, as applicable. $P < 0.05$ was considered significant.

Results

Clinical assessment and genetic testing in family members

Further clinical analyses and genetic testing were performed in relatives of the index case (Fig. 2a). The mother of the index case (II.1) is an asymptomatic mutation carrier who does not exhibit the phenotype in the ECG at rest. The toddler (IV.1) of the young woman has a QTc prolongation of 495 ms during sleep, but the echocardiogram is normal (Fig. 2b). The brother of the deceased (III.2), also an asymptomatic mutation carrier, exhibits important QTc prolongation at night (QTc 500–540 ms) (Fig. 2c). Further inquiry in the family revealed that a maternal aunt (II.2) of the index case is an asymptomatic mutation carrier with a history of palpitations, a prolonged QTc of 560 ms in the ECG and intermittent atrioventricular block (AVB) Mobitz II (Fig. 2d). One of

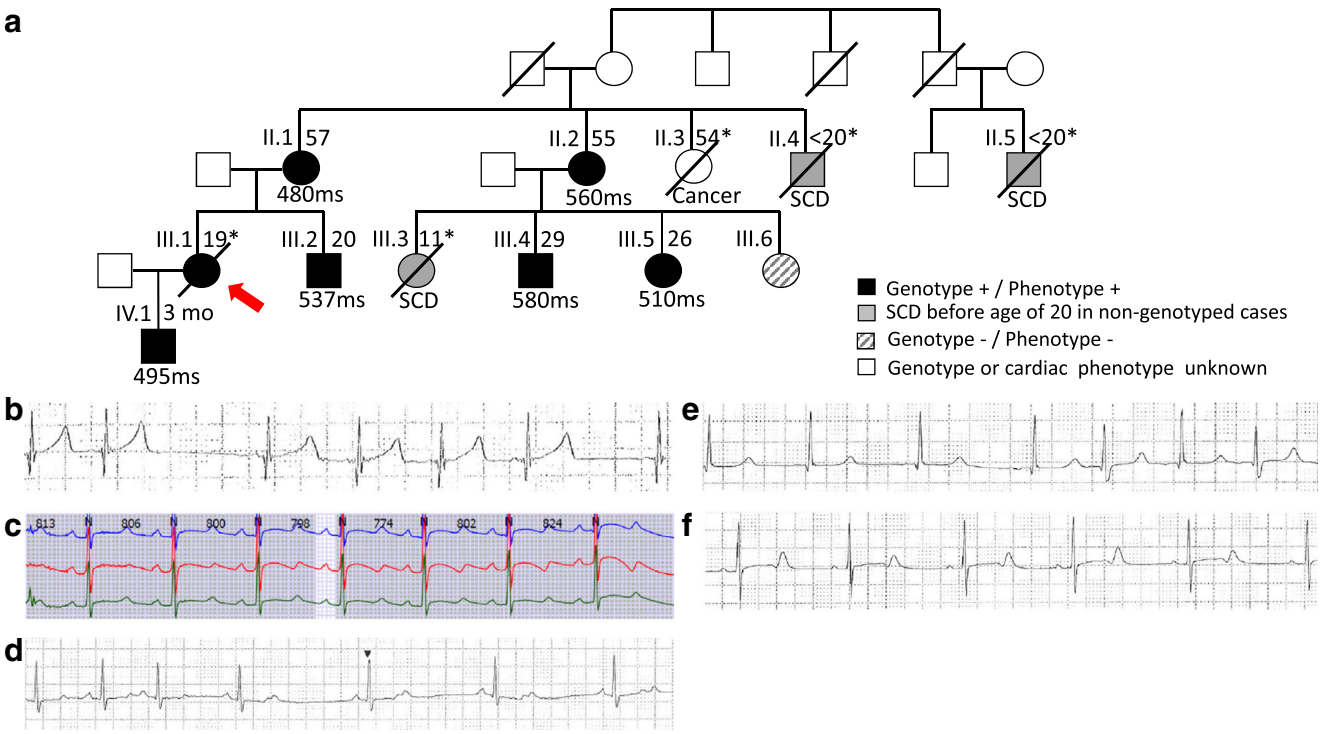

Fig. 2 Pedigree and ECG's of the investigated family. **a** Four-generation pedigree showing the individuals evaluated and the genotype or phenotype observed. Red arrow: initial index case, in which the *SCN5A* N1774H variant was detected for the first time. QTc values are shown below each individual. Ages at clinical evaluation are shown above each individual. A single asterisk indicates age at sudden death. **b-f** 12-lead resting ECG (sweep speed 25 mm/s, 10 mm/mV) of **b** the son (IV.1) of the index case, **c** the brother (III.2), **d** the aunt (II.2), **e** the cousin (III.4) and **f** the second cousin (III.5). SCD, sudden cardiac death; mo, months. (For interpretation of the references to colour in this figure legend, the reader is referred to the online version of the article)

her daughters (III.3) died suddenly at the age of 11 while climbing up a bar during school sports class without any previous symptoms or any suspected diseases. Post-mortem examination designated the case as an autopsy-negative sudden unexplained death. Unfortunately, there was no more tissue available to perform genetic testing for this study. This aunt (II.2) has two more daughters and one son, all asymptomatic. The son (III.4), although asymptomatic until now, is a carrier of the sequence alteration and exhibits significant QTc prolongation, particularly at night, with measurements reaching 600 ms (Fig. 2e). One of the two daughters (III.5), also a mutation carrier, exhibits QTc prolongation of 510 ms (Fig. 2f). The other daughter (III.6) does not carry the variant and the QTc is normal. Due to the high risk of sudden cardiac death in individuals II.2, III.4 and III.5, a cardiac implantable defibrillator was offered and implanted as primary prevention.

SCN5A N1774H decreases peak current density but increases late current

In the homozygous state, the TsA-201 cell line transiently transfected with N1774H variant reveals a significant decrease (around 48 %) of the peak current densities mediated by the variant compared to the WT (Fig. 3a, b; Table 1). In addition, main biophysical properties of N1774H (steady-state inactivation (SSI) and activation (SSA) curves) are significantly shifted compared to $Na_v1.5$ WT channels (Fig. 3c; Table 1). The SSI curve of N1774H is significantly shifted by − 3.5 mV in a hyperpolarizing direction, while the SSA curve is shifted by + 3.8 mV in a depolarizing direction.

To mimic the heterozygous state, the co-transfection of the $Na_v1.5$ WT and N1774H was performed at the ratio of 1:1. In the same experiment, we also repeated the transfection with either $Na_v1.5$ WT or N1774H. In this case, the peak current densities have been recorded with a lower sodium ion concentration (25 mmol/L instead of 50 mmol/L) in the bath solution due to the high sensitivity of the amplifier. Consistent with the results in the homozygous state, the peak current densities of homozygous N1774H revealed a significant decrease (around 37 %) compared to $Na_v1.5$ WT, but no significant difference was observed between WT and the co-expressed WT/N1774H condition (Fig. 4a, b, and d; Table 2). These results suggest that the N1774H variant does not mediate a dominant negative effect on $Na_v1.5$ WT channels. Moreover, the SSI curve of N1774H is shifted by − 1.4 mV in a hyperpolarizing direction, while the SSA curve is shifted by + 2.1 mV in a depolarizing direction compared to WT (Fig. 4c). However, these shifts are not statistically significant probably due to our experimental conditions (e.g. smaller sodium current). Altogether, the variant N1774H consistently shows a decrease of the sodium current densities without a dominant negative effect.

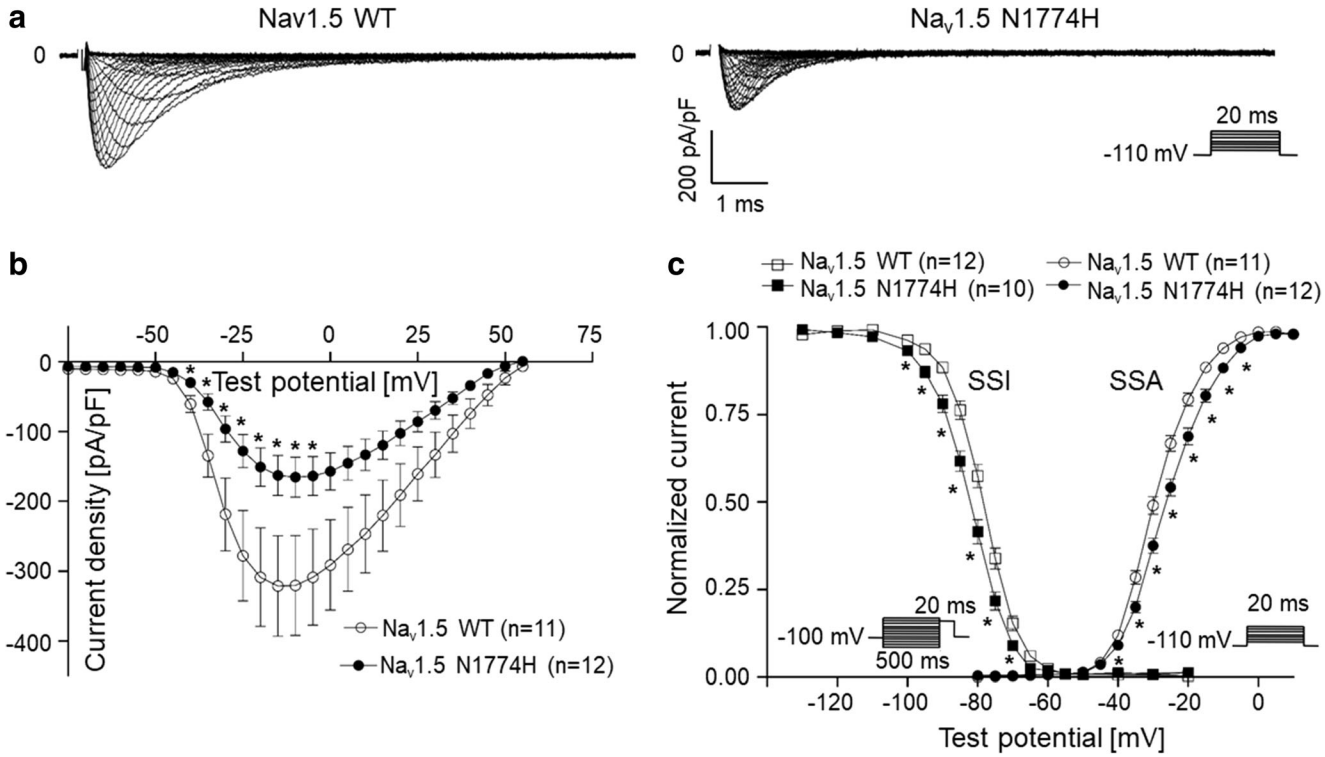

Fig. 3 **a** Representative whole-cell I_{Na} traces showing the decrease of current density with the $Na_v1.5$ N1774H variant compared to WT. **b** Current-voltage relationships (I/V) in cells transfected with either WT (white circles) or $Na_v1.5$ N1774H variant (black circles) of sodium channels (*; $p < 0.05$). **c** Steady-state inactivation (SSI, left) and activation (SSA, right) curves of either WT (white symbols) or $Na_v1.5$ N1774H variant (black symbols) of sodium channels (*; $p < 0.05$). The number of cells is indicated in parentheses

Table 1 Biophysical properties of the homozygous state $Na_v1.5$ WT and $Na_v1.5$ N1774H variant

	Sodium current density	Steady-state inactivation		Activation curve	
	I_{Na} (pA/pF)	k	$V_{1/2}$ (mV)	k	$V_{1/2}$ (mV)
$Na_v1.5$ WT	− 321 ± 75 (n = 11)	5.2 ± 0.1 (n = 12)	− 78.7 ± 0.7 (n = 12)	6.1 ± 0.2 (n = 11)	− 29.0 ± 0.7 (n = 11)
$Na_v1.5$ N1774H	− 165 ± 30 (n = 12)	5.8 ± 0.1 (n = 10)	− 82.5 ± 0.8 (n = 10)	7.0 ± 0.2 (n = 12)	− 25.5 ± 0.8 (n = 12)
P value	*	**	**	**	**

*$p < 0.05$, **$p > 0.01$; wild-type versus Nav1.5 N1774H variant. The number of cells is indicated in parentheses

Interestingly, late sodium current measurements using the non-equilibrium protocol highlight the increase of a persistent inward current with the variant N1774H (+ 363 %) compared to wild-type channels as also observed with the canonical mutation ΔKPQ used as a positive control (+ 903 %) (Fig. 5a, b).

The presence of persistent current in combination with the decrease of the peak currents suggest that the variant N1774H leads to a decrease in the peak current densities but increased the late current in the TsA-201 cell model.

N1774H has a decreased protein expression

To understand the underlying mechanism of the N1774H variant, we analysed the total $Na_v1.5$ protein expression in the total input and the surface biotinylated fraction using cell surface biotinylation assay and western blot. We observed that both $Na_v1.5$ WT and N1774H are expressed in the transient transfected TsA-201 cells. The total N1774H protein expression was reduced significantly by 51 %, and its surface expression by 24 % compared to WT (Fig. 6a, b and Supportive Figure 1). Taken together, the N1774H variant shows a decreased protein expression.

Discussion

In this case report, we describe the functional consequences of a novel *SCN5A* variant N1774H, detected in the intracellular C-terminus region of $Na_v1.5$, initially diagnosed in a 19-year-old

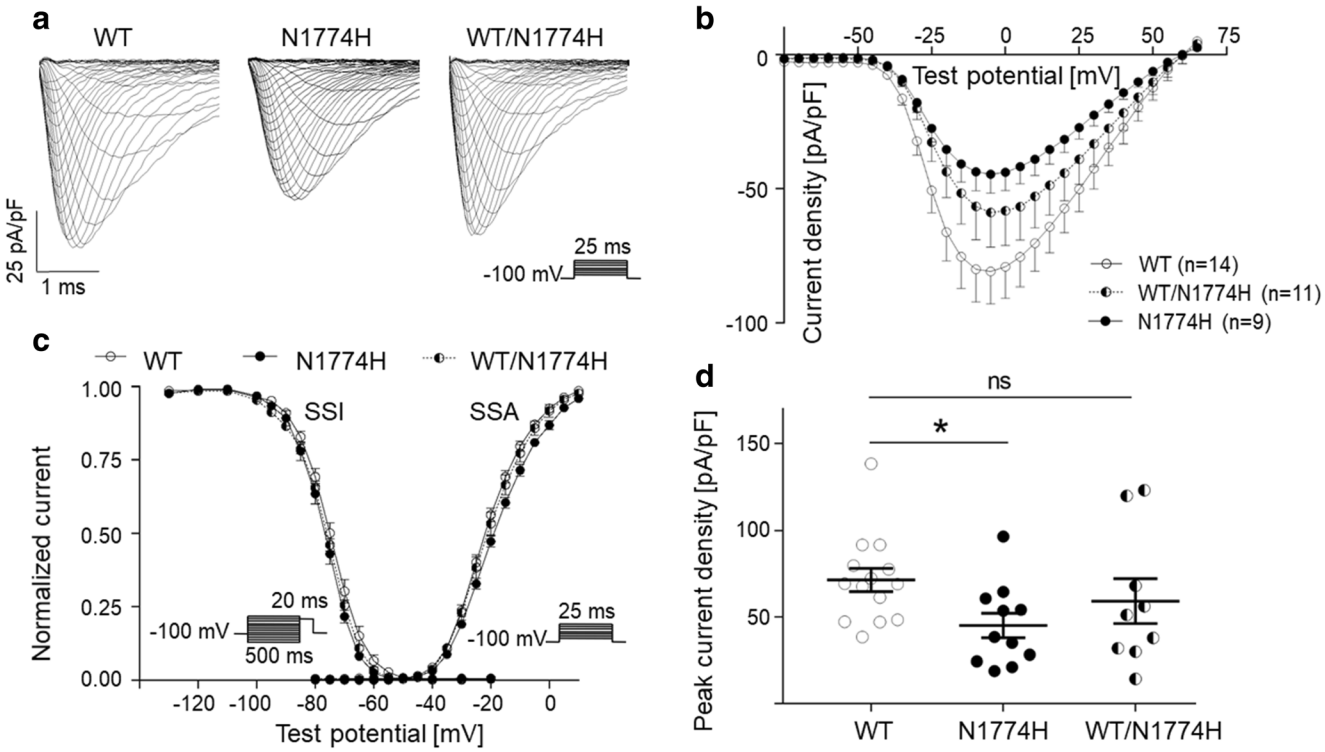

Fig. 4 **a** Representative whole-cell I_{Na} traces recorded from TsA-201 cells transiently transfected with $Na_v1.5$ WT, N1774H or co-transfected with $Na_v1.5$ WT/N1774H. **b** I/V curves show the current density and voltage relationship of the three listed conditions. **c** Steady-state inactivation (SSI, left) and activation (SSA, right) obtained using the Boltzmann equation. The whole-cell patch-clamp protocols are illustrated under the respective curves. **d** Peak current density of each condition. Data are presented as mean ± SEM, *$p < 0.05$. ns, not significant

Table 2 Biophysical properties of the heterozygous state $Na_v1.5$ WT/N1774H

	Sodium current density		Activation curve				Steady-state inactivation			
	I_{Na} (pA/pF)	*P* value	*k*	*P* value	$V_{1/2}$ (mV)	*P* value	*k*	*P* value	$V_{1/2}$ (mV)	*P* value
$Na_v1.5$ WT	− 71.3 ± 6.8 (*n* = 14)		7.7 ± 0.3 (*n* = 10)		− 20.3 ± 0.8 (*n* = 10)		5.8 ± 0.2 (*n* = 14)		− 76.0 ± 1.0 (*n* = 14)	
$Na_v1.5$ N1774H	− 45.0 ± 7.1 (*n* = 11)	*	8.2 ± 0.1 (*n* = 10)	ns	− 18.2 ± 0.7 (*n* = 10)	ns	5.6 ± 0.2 (n = 10)	ns	− 77.4 ± 1.0 (*n* = 10)	ns
$Na_v1.5$ WT/N1774H	− 59.1 ± 13.0 (*n* = 9)	ns	7.5 ± 0.2 (*n* = 9)	ns	− 20.3 ± 1.3 (*n* = 9)	ns	6.2 ± 0.2 (*n* = 10)	ns	− 76.7 ± 0.6 (*n* = 10)	ns

*$p < 0.05$ $Na_v1.5$ WT versus $Na_v1.5$ N1774H or $Na_v1.5$ WT/N1774H. The number of cells is indicated in parentheses. ns, not significant

female SADS victim. The electrophysiological characterisation revealed a significant loss-of-function for the peak current density but an increased late current compared to $Na_v1.5$ WT channels. The main clinical phenotype observed in this family was long QT syndrome (LQTS), which might be due to the increase of the late sodium current. Moreover, one patient exhibited also AVB Mobitz II, which can be the consequence of a loss-of-function mediated by the N1774H variant. We showed the co-segregation with the disease and channel function affection, which will reclassify the variant as likely pathogenic, based on the ACMG guidelines.

In general, phenotypes in *SCN5A* mutation carriers are highly diverse, which in part can be explained by the fact that different biophysical aspects of the channel could be affected by the variant, leading to various arrhythmia syndromes such as long QT syndrome type 3 (LQT3), Brugada syndrome (BrS), conduction disease, sick sinus syndrome, atrial fibrillation, atrial standstill and sudden infant death syndrome [18, 19]. It is interesting that several sequence alterations in the C-terminus region of $Na_v1.5$ display mixed phenotypes, known as cardiac sodium channel overlap syndromes [20]. The most common mutation in *SCN5A* associated with BrS and LQT3 is the E1784K variant and is classically associated with both phenotypes in vitro and clinically [21, 22]. Another amino acid replacement N1774D at the same position as the here investigated variant N1774H has recently been described in a 1-day-old boy with a prolonged heart rate corrected QT intervals (QTc) of 680 ms and familial history of sudden death in infancy [23]. Functional characterization of N1774D displayed tetrodotoxin-sensitive-persistent late sodium current leading to a gain-of-function. In addition, the same amino acid replacement has been reported in a male foetus with typical clinical signs of LQT3 involving convulsion, ventricular tachycardia, torsade de pointes, AVB and QTc interval of 670 ms [24]. Also in the C-terminus, very close to our reported variant, is the founder mutation *SCN5A*-1795insD reported in several Dutch families, characterised by electrocardiographic features of LQTS, BrS and/or progressive cardiac conduction defects [25]. However, it is still unclear why some variant carriers exhibit predominantly one phenotype despite that in vitro both are equally important. Usually, LQTS is the predominant phenotype, whereas BrS appears with age [26]. These cardiac sodium channel overlap syndromes have important therapeutic implications since some patients with a gain-of-function phenotype may benefit from sodium channel blockers treatment, whereas patients hosting variants exhibiting a loss-of-function phenotype in vitro may have a higher risk to develop arrhythmias when treated with sodium channel blockers [27, 28].

This case report of a young SADS victim illustrates the importance of post-mortem genetic testing in combination with family screening and functional characterization of the identified variant in order to understand the underlying mechanism possibly leading to the sudden death event. Notably, many variants, which were initially reported as pathogenic, may have been

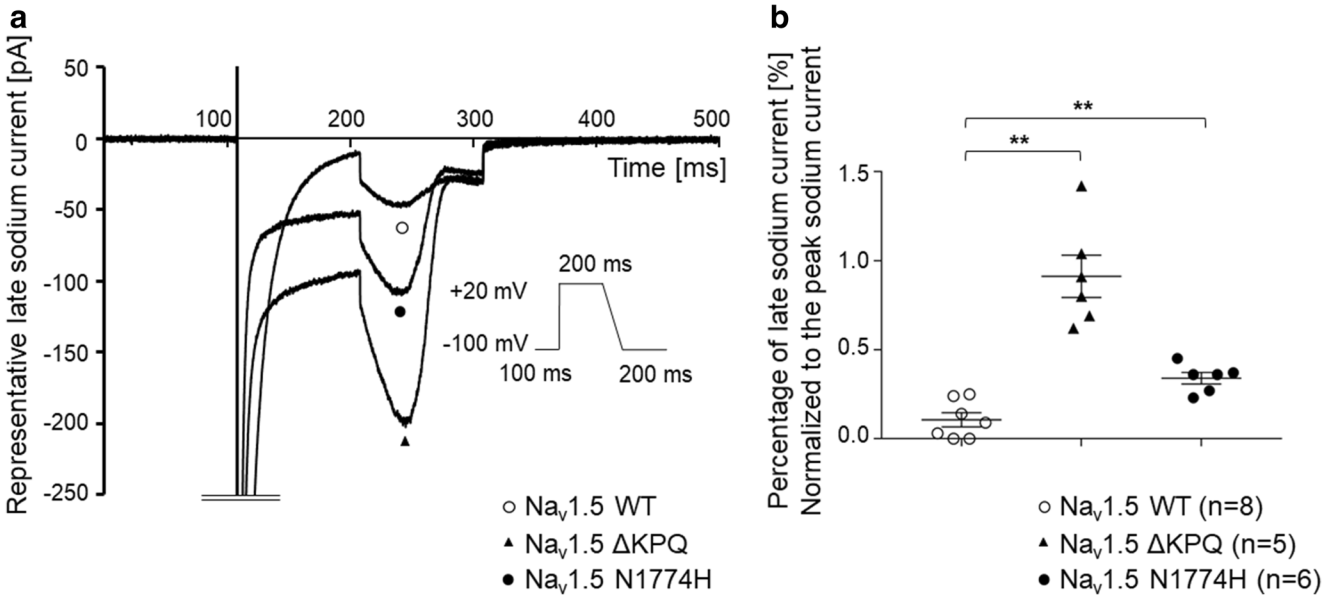

Fig. 5 **a** Representative whole-cell I_{Na} traces showing the late current using non-equilibrium protocol with the $Na_v1.5$ N1774H and ΔKPQ variants compared to WT. **b** Dot plot showing the significant increase, compared to WT condition (white circles), of the persistent current due to either the deletion of KPQ amino acid (black triangles) or the point mutation of the $Na_v1.5$ channel N1774H (black circles) (*; $p < 0.05$). The number of cells is indicated in parentheses

classified erroneously and show only little or no functional effects [29]. Furthermore, accurate investigations are crucial to identify additional family members at risk in whom death-predisposing disorders had remained unrecognized so far.

The patch-clamp analysis of $Na_v1.5$ N1774H showed a loss-of-function in peak current densities. The hyperpolarizing shift in SSI and the depolarizing shift in SSA curves indicate that less N1774H channels are available compared to $Na_v1.5$ WT at a given test potential. The loss-of-function in the peak current densities is consistent with our biochemistry experiment results, in which N1774H shows a decreased protein expression in TsA-201 cells. This indicates that the underlying mechanism of the loss-of-function is due to the decreased N1774H protein expression. Furthermore, N1774H does not negatively regulate the channel function when co-expressed with $Na_v1.5$ WT, suggesting that N1774H exerts no dominant negative effect [30]. Nevertheless, we also observed an increased late current in N1774H compared to WT channels. The underlying mechanism

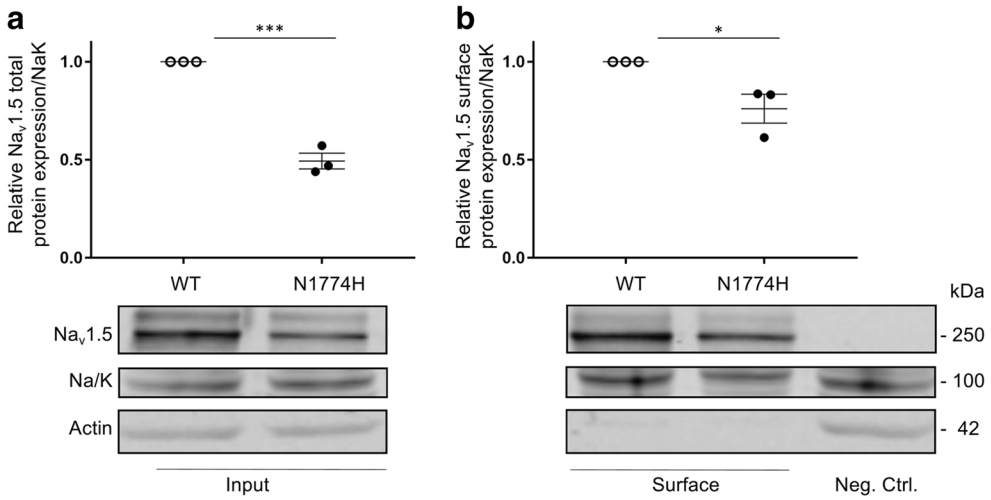

Fig. 6 $Na_v1.5$ protein expression analysis. TsA-201 cells were transiently transfected with $Na_v1.5$ WT and N1774H. **a** Upper panel: statistical analysis of western blots with input showed that the $Na_v1.5$ protein expression of N1774H was significantly decreased compared to WT; lower panel: representative western blot with input. **b** Upper panel: statistical analysis of western blots with surface showed that the $Na_v1.5$ protein expression of N1774H was significantly decreased compared to WT; lower panel: representative western blot with the surface. Data are represented as relative $Na_v1.5$ protein expression ± SEM. ***$p = 0.0002$ and $p = 0.0319$. Sodium potassium ATPase (Na/K) served as a positive loading control in both total cell lysates (input) and in surface biotinylated fraction (surface). Actin served as a positive loading control in input and at the same time as a negative loading control in the surface

of the increased late current has been reported as the physiological modulator alterations such as Ca^{2+}, calmodulin and phosphorylation [31]. A recent publication shows strong evidence that the increased late current is due to the impaired $Na_v1.5$ C-terminus to the inactivation gate by disease-causing mutations [32]. Taken together, our data strongly suggest that N1774H may lead to a potential overlap syndrome.

Based on the limitations due to the experimental model used in this investigation (TsA-201 cell line), the functional consequences of this variant in native cardiomyocytes might be different. In fact, in cardiac cells, contrary to the TsA-201 cell line, $Na_v1.5$ channels are mainly expressed in specific structures within macro-molecular complexes allowing specific regulation of the voltage-gated sodium channel. Further investigations using another model close to cardiomyocytes such as cardiomyocytes derived from *induced pluripotent stem* (iPS) *cells* from the patients could be an alternative to decipher how pathogenic this variant is. Another limitation is that the second *SCN5A* variant H558R was not included in the electrophysiological experiments with N1774H. Although H558R is the most common polymorphism in *SCN5A*, the role of this polymorphism on other variants within *SCN5A* is not fully understood [15]. Some studies have shown mitigating or aggravating effects on other mutations. Other studies did not show significant effects on the phenotype of *SCN5A*-E161K and *SCN5A*-E1784K carriers [21, 33]. Nevertheless, additional investigations are required to further validate the possible influence of the H558R polymorphism on N1774H.

Conclusion

We conclude that there is strong clinical evidence and in vitro functional data to consider the reported *SCN5A* variant N1774H as disease-causing, with a predominant clinical phenotype of long QT syndrome and sudden cardiac death.

Funding This work was supported by the Swiss Heart Foundation and the Swiss National Science Foundation SNF (project nos. 310030_165741 and 320030_149456).

Compliance with ethical standards

All procedures performed in studies involving human participants were in accordance with the ethical standards of the institutional and/or national research committee and with the 1964 Helsinki Declaration and its later amendments or comparable ethical standards.

Conflict of interest The authors declare that they have no conflict of interest.

Statement of informed consent All available family members signed an informed consent form for co-segregation analysis and gave approval for publication of this case report (Cantonal Ethics Committee Bern (KEK-BE-Nr. 2016-01602)).

References

1. Ackerman MJ, Priori SG, Willems S, Berul C, Brugada R, Calkins H, Camm AJ, Ellinor PT, Gollob M, Hamilton R, Hershberger RE, Judge DP, Le Marec H, McKenna WJ, Schulze-Bahr E, Semsarian C, Towbin JA, Watkins H, Wilde A, Wolpert C, Zipes DP, Heart Rhythm S, European Heart Rhythm A (2011) HRS/EHRA expert consensus statement on the state of genetic testing for the channelopathies and cardiomyopathies: this document was developed as a partnership between the Heart Rhythm Society (HRS) and the European Heart Rhythm Association (EHRA). Europace 13(8):1077–1109. https://doi.org/10.1093/europace/eur245
2. Basso C, Aguilera B, Banner J, Cohle S, d'Amati G, de Gouveia RH, di Gioia C, Fabre A, Gallagher PJ, Leone O, Lucena J, Mitrofanova L, Molina P, Parsons S, Rizzo S, Sheppard MN, Mier MPS, Kim Suvarna S, Thiene G, van der Wal A, Vink A, Michaud K, Association for European Cardiovascular P (2017) Guidelines for autopsy investigation of sudden cardiac death: 2017 update from the Association for European Cardiovascular Pathology. Virchows Arch 471(6):691–705. https://doi.org/10.1007/s00428-017-2221-0
3. Cerrone M, Priori SG (2011) Genetics of sudden death: focus on inherited channelopathies. Eur Heart J 32(17):2109–2118. https://doi.org/10.1093/eurheartj/ehr082
4. Narula N, Tester DJ, Paulmichl A, Maleszewski JJ, Ackerman MJ (2014) Post-mortem whole exome sequencing with gene-specific analysis for autopsy-negative sudden unexplained death in the young: a case series. Pediatr Cardiol 36(4):768–778. https://doi.org/10.1007/s00246-014-1082-4
5. Hertz CL, Christiansen SL, Ferrero-Miliani L, Fordyce SL, Dahl M, Holst AG, Ottesen GL, Frank-Hansen R, Bundgaard H, Morling N (2015) Next-generation sequencing of 34 genes in sudden unexplained death victims in forensics and in patients with channelopathic cardiac diseases. Int J Legal Med 129(4):793–800. https://doi.org/10.1007/s00414-014-1105-y
6. Anderson JH, Tester DJ, Melissa L, Ackerman MJ (2016) Whole-exome molecular autopsy after exertion-related sudden unexplained death in the young. Circ Cardiovasc Genet 9(3):260–265. https://doi.org/10.1161/CIRCGENETICS.115.001370
7. Bagnall RD, Weintraub RG, Ingles J, Duflou J, Yeates L, Lam L, Davis AM, Thompson T, Connell V, Wallace J, Naylor C, Crawford J, Love DR, Hallam L, White J, Lawrence C, Lynch M, Morgan N, James P, du Sart D, Puranik R, Langlois N, Vohra J, Winship I, Atherton J, McGaughran J, Skinner JR, Semsarian C (2016) A prospective study of sudden cardiac death among children and young adults. N Engl J Med 374(25):2441–2452. https://doi.org/10.1056/NEJMoa1510687
8. Christiansen SL, Hertz CL, Ferrero-Miliani L, Dahl M, Weeke PE, Camp L, Ottesen GL, Frank-Hansen R, Bundgaard H, Morling N (2016) Genetic investigation of 100 heart genes in sudden unexplained death victims in a forensic setting. Eur J Hum Genet 24(12):1797–1802. https://doi.org/10.1038/ejhg.2016.118
9. Lahrouchi N, Raju H, Lodder EM, Papatheodorou E, Ware JS, Papadakis M, Tadros R, Cole D, Skinner JR, Crawford J, Love DR, Pua CJ, Soh BY, Bhalshankar JD, Govind R, Tfelt-Hansen J, Winkel BG, van der Werf C, Wijeyeratne YD, Mellor G, Till J, Cohen MC, Tome-Esteban M, Sharma S, Wilde AAM, Cook SA, Bezzina CR, Sheppard MN, Behr ER (2017) Utility of post-mortem genetic testing in cases of sudden arrhythmic death syndrome. J Am Coll Cardiol 69(17):2134–2145. https://doi.org/10.1016/j.jacc.2017.02.046
10. Neubauer J, Lecca MR, Russo G, Bartsch C, Medeiros-Domingo A, Berger W, Haas C (2018) Exome analysis in 34 sudden unexplained death (SUD) victims mainly identified variants in channelopathy-associated genes. Int J Legal Med 132(4):1057–1065. https://doi.org/10.1007/s00414-018-1775-y

11. Shanks GW, Tester DJ, Ackerman JP, Simpson MA, Behr ER, White SM, Ackerman MJ (2018) Importance of variant interpretation in whole-exome molecular autopsy: population-based case series. Circulation 137(25):2705–2715. https://doi.org/10.1161/CIRCULATIONAHA.117.031053
12. Ackerman JP, Bartos DC, Kapplinger JD, Tester DJ, Delisle BP, Ackerman MJ (2016) The promise and peril of precision medicine: phenotyping still matters most. Mayo Clin Proc. https://doi.org/10.1016/j.mayocp.2016.08.008
13. Richards S, Aziz N, Bale S, Bick D, Das S, Gastier-Foster J, Grody WW, Hegde M, Lyon E, Spector E, Voelkerding K, Rehm HL, Committee ALQA (2015) Standards and guidelines for the interpretation of sequence variants: a joint consensus recommendation of the American College of Medical Genetics and Genomics and the Association for Molecular Pathology. Genet Med 17(5):405–424. https://doi.org/10.1038/gim.2015.30
14. Neubauer J, Haas C, Bartsch C, Medeiros-Domingo A, Berger W (2016) Post-mortem whole-exome sequencing (WES) with a focus on cardiac disease-associated genes in five young sudden unexplained death (SUD) cases. Int J Legal Med 130(4):1011–1021. https://doi.org/10.1007/s00414-016-1317-4
15. Gui J, Wang T, Trump D, Zimmer T, Lei M (2010) Mutation-specific effects of polymorphism H558R in SCN5A-related sick sinus syndrome. J Cardiovasc Electrophysiol 21(5):564–573. https://doi.org/10.1111/j.1540-8167.2010.01762.x
16. Zareba W, Sattari MN, Rosero S, Couderc JP, Moss AJ (2001) Altered atrial, atrioventricular, and ventricular conduction in patients with the long QT syndrome caused by the ΔKPQ SCN5A sodium channel gene mutation. Am J Cardiol 88
17. Clancy CE, Tateyama M, Liu H, Wehrens XH, Kass RS (2003) Non-equilibrium gating in cardiac Na+ channels: an original mechanism of arrhythmia. Circulation 107(17):2233–2237. https://doi.org/10.1161/01.CIR.0000069273.51375.BD
18. Remme CA, Verkerk AO, Nuyens D, van Ginneken AC, van Brunschot S, Belterman CN, Wilders R, van Roon MA, Tan HL, Wilde AA, Carmeliet P, de Bakker JM, Veldkamp MW, Bezzina CR (2006) Overlap syndrome of cardiac sodium channel disease in mice carrying the equivalent mutation of human SCN5A-1795insD. Circulation 114(24):2584–2594. https://doi.org/10.1161/CIRCULATIONAHA.106.653949
19. Makita N (2009) Phenotypic overlap of cardiac sodium channelopathies: indiviudal-specific or mutation-specific? Circ J 73:810–817
20. Remme CA, Wilde AA, Bezzina CR (2008) Cardiac sodium channel overlap syndromes: different faces of SCN5A mutations. Trends Cardiovasc Med 18(3):78–87. https://doi.org/10.1016/j.tcm.2008.01.002
21. Veltmann C, Barajas-Martinez H, Wolpert C, Borggrefe M, Schimpf R, Pfeiffer R, Caceres G, Burashnikov E, Antzelevitch C, Hu D (2016) Further insights in the most common SCN5A mutation causing overlapping phenotype of long QT syndrome, Brugada syndrome, and conduction defect. J Am Heart Assoc 5(7). https://doi.org/10.1161/JAHA.116.003379
22. Makita N, Behr E, Shimizu W, Horie M, Sunami A, Crotti L, Schulze-Bahr E, Fukuhara S, Mochizuki N, Makiyama T, Itoh H, Christiansen M, McKeown P, Miyamoto K, Kamakura S, Tsutsui H, Schwartz PJ, George AL Jr, Roden DM (2008) The E1784K mutation in SCN5A is associated with mixed clinical phenotype of type 3 long QT syndrome. J Clin Invest 118(6):2219–2229. https://doi.org/10.1172/JCI34057
23. Kato K, Makiyama T, Wu J, Ding WG, Kimura H, Naiki N, Ohno S, Itoh H, Nakanishi T, Matsuura H, Horie M (2014) Cardiac channelopathies associated with infantile fatal ventricular arrhythmias: from the cradle to the bench. J Cardiovasc Electrophysiol 25(1):66–73. https://doi.org/10.1111/jce.12270
24. Horigome H, Nagashima M, Sumitomo N, Yoshinaga M, Ushinohama H, Iwamoto M, Shiono J, Ichihashi K, Hasegawa S, Yoshikawa T, Matsunaga T, Goto H, Waki K, Arima M, Takasugi H, Tanaka Y, Tauchi N, Ikoma M, Inamura N, Takahashi H, Shimizu W, Horie M (2010) Clinical characteristics and genetic background of congenital long-QT syndrome diagnosed in fetal, neonatal, and infantile life: a nationwide questionnaire survey in Japan. Circ Arrhythm Electrophysiol 3(1):10–17. https://doi.org/10.1161/CIRCEP.109.882159
25. Postema PG, Van den Berg MP, Van Tintelen JP, Van den Heuvel B, Grundeken M, Hofman N, Van der Roest WP, Nannenberg EA, Krapels IPC, Bezzina CR, Wilde AAM (2009) Founder mutations in the Netherlands: SCN5A 1795insD, the first described arrhythmia overlap syndrome and one of the largest and best characterised families worldwide. Neth Hear J 17(11):422–428
26. Beaufort-Krol GC, van den Berg MP, Wilde AA, van Tintelen JP, Viersma JW, Bezzina CR, Bink-Boelkens MT (2005) Developmental aspects of long QT syndrome type 3 and Brugada syndrome on the basis of a single SCN5A mutation in childhood. J Am Coll Cardiol 46(2):331–337. https://doi.org/10.1016/j.jacc.2005.03.066
27. Mazzanti A, Maragna R, Faragli A, Monteforte N, Bloise R, Memmi M, Novelli V, Baiardi V, Baiardi P, Etheridge SP, Napolitano C, Priori SG (2016) Gene-specific therapy with mexiletine reduces arrhythmic events in patients with long QT syndrome type 3. J Am Coll Cardiol 67(9):1053–1058
28. Nakaya H (2014) SCN5A mutations associated with overlap phenotype of long QT syndrome type 3 and Brugada syndrome. Circ J 78(5):1061–1062. https://doi.org/10.1253/circj.CJ-14-0319
29. Andreasen C, Nielsen JB, Refsgaard L, Holst AG, Christensen AH, Andreasen L, Sajadieh A, Haunso S, Svendsen JH, Olesen MS (2013) New population-based exome data are questioning the pathogenicity of previously cardiomyopathy-associated genetic variants. Eur J Hum Genet 21(9):918–928. https://doi.org/10.1038/ejhg.2012.283
30. Hübner CA, Jentsch TJ (2002) Ion channel diseases. Hum Mol Genet 11:2435–2445
31. Moreno JD, Clancy CE (2012) Pathophysiology of the cardiac late Na current and its potential as a drug target. J Mol Cell Cardiol 52(3):608–619. https://doi.org/10.1016/j.yjmcc.2011.12.003
32. Gardill BR, Rivera-Acevedo RE, Tung CC, Okon M, McIntosh LP, Van Petegem F (2018) The voltage-gated sodium channel EF-hands form an interaction with the III-IV linker that is disturbed by disease-causing mutations. Sci Rep 8(1):4483. https://doi.org/10.1038/s41598-018-22713-y
33. Wilders R (2018) Cellular mechanisms of sinus node dysfunction in carriers of the SCN5A-E161K mutation and role of the H558R polymorphism. Front Physiol 9:1795. https://doi.org/10.3389/fphys.2018.01795